Int. J. Heat Mass Transfer. Vol. 15, pp. 493–502. Pergamon Press 1972. Printed in Great Britain

HEAT AND MASS TRANSFER IN SEMI-POROUS CHANNELS WITH APPLICATION TO FREEZE-DRYING

W. M. MASSEY, JR.
E. I. DuPont de Nemours and Co., P.O. Box 71, Chattanooga, Tennessee, U.S.A.
and
J. E. SUNDERLAND
Department of Mechanical and Aerospace Engineering, North Carolina State University, Raleigh, North Carolina, U.S.A.

(*Received* 14 *January* 1971 *and in revised form* 21 *May* 1971)

Abstract—An analytical investigation is made of the heat and momentum transfer of a binary mixture of gases flowing in a parallel plate channel where mass injection occurs at one wall. The walls are at different temperatures and applications to freeze-drying are presented. Integral continuity, momentum, and energy equations are used to establish the velocity, pressure, and temperature distributions. The flow is assumed to be steady, laminar, and incompressible. Closed form solutions are obtained for the velocity and temperature distributions.

Applications of the solution to freeze-drying show that under typical conditions 5–40 per cent of the energy transfer to the product surface occurs by convection. Thermal radiation provides the mechanism for the rest of the heat transfer.

NOMENCLATURE

a, b, c, d,	coefficients in velocity distribution;
a_1, b_1, c_1, d_1,	coefficients in temperature distribution;
c_p,	constant pressure specific heat;
H,	channel width;
ΔH,	heat of sublimation;
I,	integrated function;
k,	thermal conductivity of water-vapor;
k_d,	thermal conductivity of dried region;
L,	channel half length;
N_w,	mass flow rate;
P,	pressure;
q_c,	convection heat flux;
q_r,	radiant heat flux;
q_d,	conduction heat flux;
R,	wall or injection Reynolds number, $(v_0 H/\nu)$;
RPr,	Reynolds number times Prandtl number, $(v_0 H/\alpha)$;
T,	temperature;
u,	velocity in the x-direction;
v,	velocity in the y-direction;
x,	distance coordinate;
X_1,	dimensionless integration variable;
X_d,	dried layer thickness;
y,	distance coordinate.

Greek symbols

α,	thermal diffusivity;
β,	pressure derivative, $\partial P/\partial x$;
β_1,	pressure parameter, $(H^3\beta/\rho\nu v_0 x)$;
γ,	parameter in energy solution;

δ, porosity;
ε, thermal emissivity;
θ, dimensionless temperature ratio;
ν, kinematic viscosity;
ξ, dimensionless space coordinate, y/H;
ρ, density;
σ, Stefan–Boltzmann constant;
τ, time.

Subscripts
d, interface position;
f, frozen region;
LH, position on solid wall at $x = \pm L$ and $y = H$;
m, mean value;
n, integer;
0, surface of porous wall;
1, solid wall position;
2, channel exit;
3, channel exit;
e, channel exit.

INTRODUCTION

A NUMBER of investigations have been reported for the transport processes involved in porous channels. One of the earliest studies, by Berman [1], was an analytical investigation of flow in a fully porous channel. Donoughe [2], Terrill [3] and Terrill and Shrestha [4], studied a channel with one porous wall, the semi-porous channel. Studies for other geometries have been reported in [5–8].

One very important application of heat and mass transfer problems in semi-porous channels occurs in the freeze-drying of foods. In this process frozen food is placed on large trays in a vacuum chamber and heated from above as shown in Fig. 1. The region between the product surface and the heater is the semi-porous channel. For industrial applications, the space between the heater and the product surface is 0·25–1·0 in. This space is needed for handling purposes and to provide space for the vapor to flow to the condenser as shown in Fig. 2. The vapor is transported by convection and diffusion. Heat transfer to the product surface occurs by convection and radiation. Efforts at improving the rate of heat transfer to the product have been presented in [9–13].

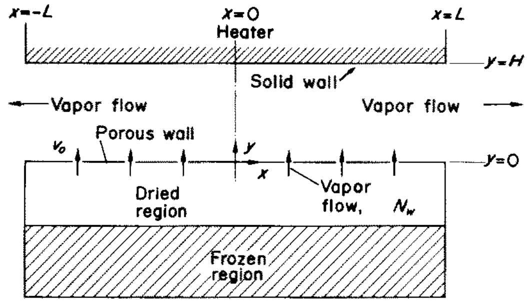

FIG. 1. Semi-porous channel.

The current study is made for the purpose of obtaining a better understanding of the transport processes and predicting the rate of heat transfer from the heated surface to the surface of the porous wall. The physical model involves a channel of length $2L$, width H and infinite depth. The porous wall represents the food surface. Integral equations are used to determine the pressure, velocity and temperature distributions in the channel. Due to the low density of the water, the Reynolds number is small; therefore, the flow is assumed to be laminar. Since freeze-drying is a very slow process, quasi-steady solutions of the transport equations are employed in this paper.

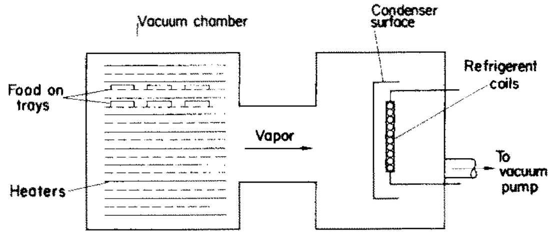

FIG. 2. Typical freeze-drying apparatus.

ANALYTICAL INVESTIGATION

Velocity distribution

The momentum equation is solved assuming that the flow is in the continuous regime, there is no flow at $x = 0$ in the x-direction (see Fig. 1), and due to symmetry $\partial P/\partial x = 0$ at $x = 0$. One dimensional solutions for the heat and mass transfer in a porous region have been determined by Dyer *et al.* [14] and Hill *et al.* [15]. So that these solutions can be used with the current investigation, it is necessary that the injection velocity at $y = 0$ be constant with respect to the x-direction. At $y = H$ the wall is impermeable.

The integral form of the momentum equation in the x-direction given by Massey [17] is

$$2\int_0^1 u\frac{\partial u}{\partial x}\,\mathrm{d}\xi = -\frac{1}{\rho}\frac{\partial P}{\partial x} + \nu\int_0^1 \frac{\partial^2 u}{\partial x^2}\,\mathrm{d}\xi + \frac{\nu}{H^2}\frac{\partial u}{\partial \xi}\bigg|_1 - \frac{\nu}{H^2}\frac{\partial u}{\partial \xi}\bigg|_0. \tag{1}$$

The velocity distribution in the x-direction is approximated by

$$u(x,\xi) = a(x) + b(x)\,H\xi + c(x)\,H^2\xi^2 + d(x)\,H^3\xi^3 \tag{2}$$

where the coefficients a, b, c and d are determined from the following conditions:

$$u(x,0) = 0 \quad \text{at} \quad \xi = 0 \tag{3}$$

$$\frac{v_0}{H}\frac{\partial u}{\partial \xi} = -\frac{1}{\rho}\frac{\partial P}{\partial x} + \frac{\nu}{H^2}\frac{\partial^2 u}{\partial \xi^2} \quad \text{at} \quad \xi = 0 \tag{4}$$

$$u(x,1) = 0 \quad \text{at} \quad \xi = 1 \tag{5}$$

and the continuity equation

$$v_0 = H\frac{\partial}{\partial x}\int_0^1 u(x,\xi)\,\mathrm{d}\xi. \tag{6}$$

Equation (4) is determined by applying the differential form of the momentum equation at the porous surface and represents a restriction placed on the velocity profile. Solving equations (2)–(6), the velocity distribution can be expressed by

$$u(x,\xi) = \frac{v_0 x}{H}\left\{\left(\frac{24-\beta_1}{R+6}\right)\xi + \left(\frac{12R+3\beta_1}{R+6}\right)\xi^2 + \left(\frac{-12R-24-2\beta_1}{R+6}\right)\xi^3\right\}. \tag{7}$$

Substituting equation (7) into equation (1) yields an ordinary differential equation with variable coefficients which can be solved using an infinite series solution. The result for β_1 is

$$\beta_1 = -\frac{\frac{214}{35} + \frac{39}{70}R + \frac{18}{R}}{\frac{1}{105}} \pm \left\{\left(\frac{\frac{214}{35} + \frac{39}{70}R + \frac{18}{R}}{\frac{1}{105}}\right)^2 - \left(\frac{\frac{48}{35}R^2 + \frac{738}{35}R + \frac{4056}{35} + \frac{216}{R}}{\frac{1}{210}}\right)\right\}^{\frac{1}{2}} \tag{8}$$

where the last term is positive for injection and negative for suction.

The velocity distribution given by equations (7) and (8) gives results within 0·1 per cent of more accurate solutions obtained by the numerical techniques of Donoughe [2] provided $R \leqslant 3$. For freeze-drying applications, this condition is easily satisfied.

Temperature distribution

To determine the temperature distribution, the integral form of the energy equation is used:

$$\int_0^1 \frac{\partial(uT)}{\partial x}\,\mathrm{d}\xi - \frac{v_0 T_0}{H} = \frac{\alpha}{H^2}\frac{\partial T}{\partial \xi}\bigg|_{\xi=1} - \frac{\alpha}{H^2}\frac{\partial T}{\partial \xi}\bigg|_{\xi=0}. \tag{9}$$

The temperature distribution is approximated by

$$T(x,\xi) = a_1(x) + b_1(x)H\xi + c_1(x)H^2\xi^2 + d_1(x)H^3\xi^3. \quad (10)$$

The following conditions may be applied to the temperature distribution:

$$T(x,0) = T_0 \quad \text{at} \quad \xi = 0 \quad (11)$$

$$T(L,1) = T_{LH} \quad (12)$$

$$\frac{v_0}{H}\frac{\partial T}{\partial \xi} = \frac{\alpha}{H^2}\frac{\partial^2 T}{\partial \xi^2} \quad \text{at} \quad \xi = 0 \quad (13)$$

$$\frac{\partial^2 T}{\partial \xi^2} = 0 \quad \text{at} \quad \xi = 1. \quad (14)$$

Equation (11) results from the assumption that the porous surface of the channel is isothermal. Equations (13) and (14) are obtained by applying the differential forms of the energy equation at the two surfaces of the channel and represent restrictions placed on the temperature profile.

By substituting the velocity distribution given by equations (7) and (8) into equation (9), then using (9), (11), (13) and (14) the coefficients for the temperature distribution in equation (10) can be determined. Equation (12) specifies a point temperature on the solid surface and is used to evaluate an integration constant which arises as a result of using equation (9). Thus

$$\frac{T(x,\xi) - T_0}{T_{LH} - T_0} = \theta(x,\xi) = \left(\frac{x}{L}\right)^{-\gamma} \times \left(\frac{3}{3 + RPr}\xi + \frac{3RPr}{6 + 2RPr}\xi^2 - \frac{RPr}{6 + 2RPr}\xi^3\right) \quad (15)$$

where

$$\gamma = 1 - \frac{(18 + 3R)}{\left(\frac{96}{5} + \frac{18R}{5} + \frac{\beta_1}{10} + \frac{162RPr}{35} + \frac{RPr\beta_1}{28} + \frac{32R^2Pr}{35}\right)}. \quad (16)$$

Since $\gamma > 0$, the temperature calculated from equation (15) becomes infinitely large at $x = 0$. This behavior results from neglecting conduction in the x-direction in equation (9). The temperature distribution of the solid surface required to maintain a uniform porous surface temperature can then be calculated. It would be necessary to use an arrangement of surface heaters to obtain experimentally this temperature distribution. However, at the low flow rates encountered in freeze-drying, a uniform surface heater temperature would be sufficient to maintain a nearly uniform porous surface temperature.

Porous surface energy balance

For applications such as those encountered in freeze-drying, the temperature of the two walls are not independently controlled. If one temperature is given, the other can be determined by making an energy balance at the surface of the porous wall. Thus

$$q_r + q_c = q_d \quad (17)$$

where the first, second and third term represent the net radiant heat transfer to the porous surface, the heat transfer by convection and/or conduction between the heater and the surface, and the heat conduction into the porous wall, respectively. For freeze-drying applications, q_d will equal the energy absorbed by the vapors moving through the dried region plus the energy of sublimation. Transient temperature changes in the dried region yield negligible changes in the energy balance owing to the low densities and high heats of sublimation involved. These assumptions have been used successfully in [14] and [15].

From the temperature distribution of equation (15), the heat transfer between the porous wall and the fluid layer can be calculated. The mean temperature of the heater may be calculated from

$$T_m = \frac{1}{2L}\int_{-L}^{L} T(x,1)\,dx. \quad (18)$$

Combining equations (15) and (18), gives

$$q_c = -\frac{k(T_{LH} - T_0)}{H}\frac{\partial\theta}{\partial\xi}\bigg|_0 = \frac{-k(T_m - T_0)(1-\gamma)}{H} \times \left(\frac{3}{3 + RPr}\right)\left(\frac{x}{L}\right)^{-\gamma}. \quad (19)$$

The mean temperature of the heater surface, T_m, is a practical quantity to measure and to use in subsequent calculations.

The rate of heat transfer per unit area conducted away from the porous surface toward the frozen-region is given by

$$q_d = \rho_0 v_0 \, \Delta H + \rho_0 v_0 c_p (T_0 - T_d) \quad (20)$$

where ρ_0 and c_p are properties of the water vapor measured at T_0.

To calculate the radiation heat transfer to the porous wall, the heater surface and the regions surrounding the exits of the channel are assumed to be black bodies and the porous surface is assumed to be gray. Also, the water-vapor flowing in the channel is considered to be transparent to thermal radiation. By following the procedure presented by Sparrow and Cess [16], Massey [17] showed that q_r can be expressed by:

$$q_r(x_0) = \frac{\varepsilon_0}{1-\varepsilon_0}\left\{(1-\varepsilon_0)\sigma T_0^4 - (1-\varepsilon_0)\sigma \int_{x_1} \frac{T^4(x,1)\,H^2\,dx_1}{2[(x_1 - x_0)^2 + H^2]^{\frac{3}{2}}} - \frac{(1-\varepsilon_0)\sigma T_2^4}{2} \times \left[1 - \frac{(L + x_0)}{[(L+x_0)^2 + H^2]^{\frac{1}{2}}}\right] - \frac{(1-\varepsilon_0)\sigma T_3^4}{2}\left[1 - \frac{(L - x_0)}{[(L-x_0)^2 + H^2]^{\frac{1}{2}}}\right]\right\}. \quad (21)$$

By substituting equations (19)–(21) into (17) and integrating over the porous surface, from $x_0 = -L$ to $x_0 = L$, we obtain:

$$\frac{\varepsilon_0}{1-\varepsilon_0}\left\{(1-\varepsilon_0)\sigma T_0^4\left(\frac{2L}{H}\right) - \frac{(1-\varepsilon_0)\sigma H}{2}\int_{-L}^{L}\int_{-L}^{L}\frac{T^4(x,1)\,dx_1\,dx_0}{[(x_1-x_0)^2 + H^2]^{\frac{3}{2}}} - \frac{(1-\varepsilon_0)\sigma T_2^4}{2}\left[\frac{2L}{H} + 1 - \sqrt{[4(L/H)^2 + 1]}\right] - \frac{(1-\varepsilon_0)\sigma T_3^4}{2}\left[\frac{2L}{H} + 1 - \sqrt{[4(L/H)^2 + 1]}\right]\right\}$$

$$-\frac{k(T_m - T_0)}{H}\left(\frac{6}{3 + RPr}\right)\left(\frac{L}{H}\right) = 2\rho_0 v_0 \, \Delta H\left(\frac{L}{H}\right) + 2\rho_0 v_0 c_p (T_0 - T_d)\left(\frac{L}{H}\right). \quad (22)$$

Equation (22) relates the porous surface temperature, T_0, to the mean heater temperature, T_m. Provision is made for the temperatures at the two exits, T_2 and T_3 to be unequal. This equation is useful for applications where either the surface temperature or the heater temperature is specified. Thus if the heater temperature is specified the transient surface product temperature can be determined. Alternatively, if the product temperature is specified, equation (22) can be used to determine how the heater temperature should vary.

Before equation (22) can be solved, $T(x, 1)$ from equation (15) must be substituted into (22) and the integrations must be performed. The term involving the double integral in equation (22), I, becomes:

$$I = \frac{(1-\varepsilon_0)\sigma}{2}\Big\{2T_0^4\sqrt{[4(L/H)^2+1]} - 2T_0^4 + 4T_0^3(T_{LH}-T_0)I_1 + 6T_0^2(T_{LH}-T_0)^2 I_2 + 4T_0(T_{LH}-T_0)^3 I_3 + (T_{LH}-T_0)^4 I_4\Big\} \quad (23)$$

where $I_n (n = 1, 2, 3, 4)$ is defined by

$$I_n = \frac{2}{H}\left(\frac{L}{H}\right)^2 \int_0^1 \Bigg\{\frac{-X_1^{(1-n\gamma)}}{[(L/H)^2(X_1-1)^2+1]^{\frac{3}{2}}} + \frac{X_1^{(1-n\gamma)}}{[(L/H)^2(X_1+1)^2+1]^{\frac{3}{2}}} + \frac{2X_1^{(1-2n\gamma)}}{[(L/H)^2(X_1-1)^2+1]^{\frac{3}{2}}} + \frac{2X_1^{(1-2n\gamma)}}{[(L/H)^2(X_1+1)^2+1]^{\frac{3}{2}}}\Bigg\} \mathrm{d}X_1. \quad (24)$$

During freeze-drying, the flow rate decreases as the thickness of the dried porous region increases. For a particular value of R, equation (22) is applicable for a short period of time. Since R is slowly changing, it must be considered as an average injection Reynolds number during any given time period. In this work, T_0 or T_m and R are assumed to be known. In order to relate a set of flow conditions in the channel to a particular stage of the drying cycle, it is necessary to know the depth of the dried layer or the interface position, X_d. The interface position is defined as the boundary between the dried and frozen regions of the sample. The interface position and the time required to dry to a specified thickness have been determined by Dyer *et al.* [14]. Thus

$$X_d = \frac{k_d(T_0 - T_d)}{N_w[\Delta H + c_p(T_0 - T_d)]} \quad (25)$$

where k_d is the dried layer thermal conductivity and N_w is the vapor flow rate. The drying time is

$$\tau = \frac{\rho_f \delta X_d^2}{2\left[\dfrac{k_d(T_0 - T_d)}{\Delta H + c_p(T_0 - T_d)}\right]}, \quad (26)$$

where ρ_f is the density of the frozen region and δ is the porosity of the dried layer.

APPLICATIONS TO FREEZE-DRYING

Constant heater temperature

In this section the mean heater surface temperature, T_m, is treated as known and fixed with respect to time and equation (22) is solved for the product surface temperature, T_0. A range for R is selected which covers the flow rates encountered in the typical drying cycle. The results are compared with the results of Lusk *et al.* [18] who experimentally measured the thermal conductivities of haddock fish during freeze-drying. Included in their work are plots of moisture content, the product surface temperature, and the interface temperature as a function of time for constant T_m. These experiments were carefully controlled and provide an excellent comparison for the analytical solution. Tests were made on slabs 8 by 10 in. in cross section and $\frac{3}{4}$ in. and 1 in. thick. To apply our equations to their data, $L = 5$ in., $H = 0{\cdot}625$ in. and $0{\cdot}5$ in., $T_d = 440°$R, $T_m = 635°$R and $k = 0{\cdot}013$ Btu/hft°F. They determined

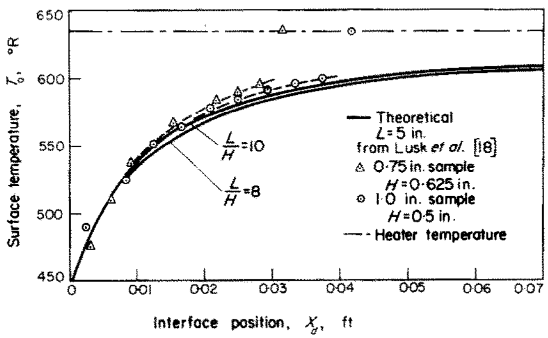

FIG. 3. Comparison of predicted and measured surface temperature of haddock during freeze-drying.

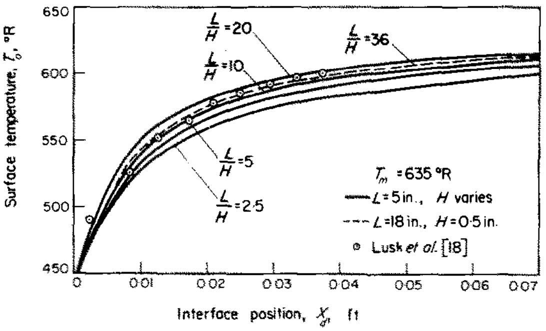

FIG. 4. Influence of channel length to width ratio on product surface temperature.

the value of thermal conductivity based on the latent heat of sublimation of pure ice (1220 Btu/lb) and a chamber pressure of 0·08 torr. The value of emissivity for haddock has not been measured, so we used a value for freeze-dried beef (0·75) from [19]. Values of the Reynolds number were generally less than 1.

The position of the interface was calculated from the data presented by Lusk *et al.* [18] for the moisture content and is presented in Fig. 3 along with the results of the current analysis. The experimental and analytical results show good agreement, especially for the one-inch thick sample.

Figure 4 shows how the product surface temperature is influenced by various ratios of L/H. This ratio is important in designing commerical freeze-dryers. The surface temperature increases slightly with increasing values of L

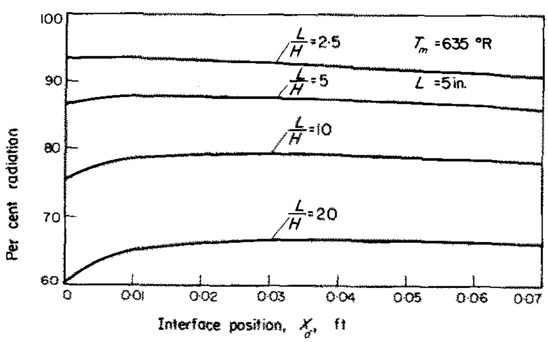

FIG. 5. Influence of channel length to width ratio on percentage of heat transfer to the product by radiation.

due to the decrease in radiation losses at the channel exits. The surface temperature increases with decreasing values of H due to convective effects. At a given interface position, a higher value of T_0 would result in a higher drying rate.

Figure 5 shows the percentage of the energy that is transferred to the product by thermal radiation. Thus 60–95 per cent of the heat transferred to the product surface is thermal radiation. The remainder is convection. The ratio of radiation to convection heat transfer depends on the L/H ratio and is nearly constant throughout a typical drying cycle.

Constant product surface temperature

In this section the product surface temperature is constant with respect to time and position. By selecting values of R, equation (22) is used to calculate a heater temperature T_m required to maintain the product surface at the prescribed temperature and flow rate. Equation (25) may be used to relate external flow conditions to the corresponding interface position. However, it is possible to go a step further in this section and use equation (26) to calculate the time to dry to a particular interface position. No experimental data is available for comparison with the analytical results for this case.

The product surface temperature, T_0, unless otherwise specified is 560°R and the total chamber pressure is one torr. The interface temperature, T_d, at one torr is 466°R. The channel exit temperature, T_e, unless otherwise specified is 530°R. The properties of freeze-dried beef are used in the following calculations. The thermal conductivity measured by Massey *et al.* [20] is 0·0503 Btu/hft°F at one torr. This is the calculated value using a heat of sublimation for freeze-dried beef given by Dyer *et al.* [21] of 1488 Btu/lb_m. The porosity of freeze-dried beef, δ, is 0·70.

Figures 6 and 7 are plots of the mean heater temperature vs. time. Figure 6 illustrates the effect on T_m of varying the channel width H for a long channel. Figure 7 is a similar plot only for a short channel. The lower heater tempera-

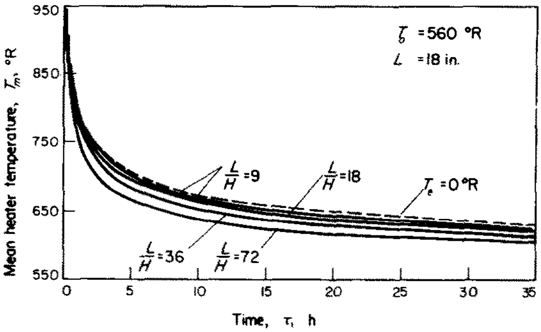

FIG. 6. Influence of channel width and exit temperature on mean heater temperature for a long channel.

ture required for the small widths is due to the increased convective heat flux across the channel and the reduced radiant heat losses for the channel exits.

Figure 7 also shows the effect of changing length L when the channel width H is held constant. The curve for $L/H = 60$ has the same channel width as the one where $L/H = 12$. The effect is small when compared with the effect a change in H has on T_m. For the practical limits of the length to width ratio encountered in practice, there is little effect as a result of varying L. This illustrates that radiant heat losses from the channel exits are very small even for relatively short channels.

Figures 6 and 7 also illustrate the influence that a change in the exit temperature has on T_m for different channel geometries. The temperature was lowered to absolute zero since this would be the minimum theoretical temperature of the surroundings. On Fig. 6 the effect of a lowered T_e is shown with the dashed line for the channel where $L/H = 9$. For the long narrow channels, there is no discernable effect on T_m. For the shorter channels of Fig. 7, the effect of a lowered T_e is shown for two L/H ratios with the dashed lines. As the geometry changes to a short wide channel, the effect becomes quite pronounced.

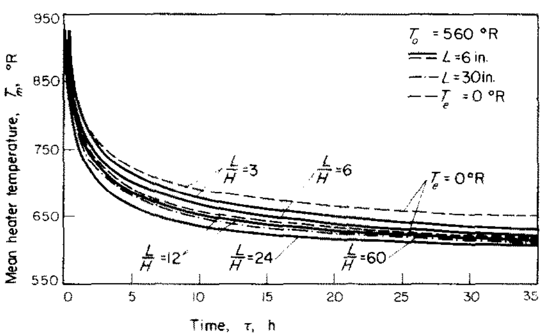

FIG. 7. Influence of channel width, length and exit temperature on mean heater temperature.

CONCLUSIONS

Based on the comparison with existing solutions, the polynomial solution for the velocity distribution in a semi-porous channel is accurate for $R \leqslant 3$. The accuracy of the polynomial solution for the temperature profile is established by comparison with published experimental results for a limited range of $RPr < 1$. The application of the semi-porous channel model to the heat transfer and fluid flow in the region between the heater platen and the food product in freeze-drying correlates well with the actual physical process since R is usually not greater than one.

In freeze-drying, it is shown that radiation heat transfer is the dominant mode of heat transfer to the product surface where an open region separates the heater and the product. Depending on the channel width, the relative amount of radiation heat transfer may range from 60 to 95 per cent of the total heat transfer to the product surface.

ACKNOWLEDGEMENTS

The writers would like to express their gratitude for the support received from Public Health Service Research Grants UI 00093-04 and UI 00712-01 from the National Center for Urban and Industrial Health and FD 00156-03 from the Food and Drug Administration.

REFERENCES

1. A. S. BERMAN, Laminar flow in channels with porous walls, *J. Appl. Phys.* **24**, 1232–1235 (1953).

2. P. L. DONOUGHE, Analysis of laminar incompressible flow in semi-porous channels, NACA TN3759 (1956).
3. R. M. TERRILL, Laminar flow in a uniformly porous channel, *Aeronaut. Q.* **15**, 299–310 (1964).
4. R. M. TERRILL and G. M. SHRESTHA, Laminar flow through parallel and uniformly porous walls of different permeability, *ZAMP* **16**, 470–482 (1965).
5. S. W. YUAN, Further investigation of laminar flow in channels with porous walls, *J. Appl. Phys.* **27**, 267–269 (1956).
6. A. S. BERMAN, Concerning laminar flow in channels with porous walls, *J. Appl. Phys.* **27**, 1557–1558 (1956).
7. E. R. G. ECKERT, P. L. DONOUGHE and B. J. MOORE, Velocity and friction characteristics of laminar viscous boundary-layer and channel flow over surfaces with ejection or suction, NACA TN4102 (1957).
8. F. M. WHITE, JR., B. F. BARFIELD and M. J. GOGLIA, Laminar flow in a uniformly porous channel, *J. Appl. Mech.* **25**, 613–617 (1958).
9. J. B. LAMBERT, Heat and mass transfer in freeze-drying, Ph.D. thesis, University of Wisconsin (1956).
10. R. F. BURKE and R. V. DECAREAU, *Advances in Food Research, XIII*, pp. 1–88. Academic Press, New York (1964).
11. I. M. ABELOW and E. W. FLOSDORF, Freeze-drying, *Chem. Engng Prog.* **53**, 597–600 (1957).
12. W. R. SMITHIES and T. S. BLAKLEY, Design of freeze-drying equipment for the dehydration of foodstuffs, *Food Technol.* **13**, 610–614 (1959).
13. G. LUSK, M. KAREL and S. A. GOLDBLITH, Effect of some processing parameters on the rates of freeze-drying of shrimp, *Food Technol.* **19**, 620–622 (1965).
14. D. F. DYER and J. E. SUNDERLAND, Heat and mass transfer mechanisms in sublimation dehydration, *J. Heat Transfer* **90C**, 379–384 (1968).
15. J. E. HILL and J. E. SUNDERLAND, Sublimation dehydration in the continuum, transition and free-molecule flow regimes, *Int. J. Heat Mass Transfer* **14**, 625–638 (1971).
16. E. M. SPARROW and R. D. CESS, *Radiation Heat Transfer*. Brooke-Cole, Belmont, Calif. (1966).
17. W. M. MASSEY, JR., Heat and mass transfer in semi-porous channels, Ph.D. Thesis, Ga. Inst. of Tech., Atlanta, Ga. (1968).
18. G. LUSK, M. KAREL and S. A. GOLDBLITH, Thermal conductivity of some freeze-dried fish, *Food Technol.* **18**, 1625–1628 (1964).
19. V. J. SEVCIK and J. E. SUNDERLAND, Emissivity of beef, *Food Technol.* **16**, 124–126 (1962).
20. W. M. MASSEY, JR and J. E. SUNDERLAND, Measurement of thermal conductivity during freeze-drying of beef, *Food Technol.* **21**, 90A–94A (1967).
21. D. F. DYER, D. K. CARPENTER and J. E. SUNDERLAND, Equilibrium vapor pressure of frozen bovine muscle, *J. Food Sci.* **31**, 196–201 (1966).

TRANSFERT THERMIQUE ET MASSIQUE DANS DES CANAUX SEMI-POREUX AVEC APPLICATION À LA LYOPHILISATION

Résumé—On mène une recherche analytique sur le transfert de chaleur et de quantité de mouvement d'un mélange binaire de gaz s'écoulant dans un canal à section rectangulaire avec injection massique par une paroi. Les parois sont à des températures différentes. On présente des applications à la lyophilisation. Les équations de continuité, de quantité de mouvement et d'énergie sont utilisées pour établir les distributions de vitesse, de pression et de température. On suppose l'écoulement permanent laminaire et le fluide incompressible. Des solutions sous forme analytique sont obtenues pour les distributions de vitesse et de température.

Des applications de la solution à la lyophilisation montrent que sous des conditions typiques 5 à 40 pour cent du transfert de l'énergie à la surface active est dû à la convection. Un rayonnement thermique contribue au mécanisme pour le reste du transfer thermique.

WÄRME- UND STOFFÜBERTRAGUNG IN HALB-PORÖSEN KANÄLEN MIT ANWENDUNG AUF DIE GEFRIERTROCKNUNG

Zusammenfassung—Mit einer binären Gasmischung wurde der Wärme- und Stoffaustausch analytisch untersucht, für Strömung in einem Kanal aus parallelen Platten, mit Stoffzufuhr von einer Wand. Die Wände haben verschiedene Temperaturen, und die Anwendung auf die Gefriertrocknung wird angegeben. Die integralen Kontinuitäts-, Impuls- und Energie-Gleichungen werden benutzt, um die Geschwindigkeits-, Druck- und Temperaturverteilungen zu erhalten. Die Strömung wird als stetig, laminar und inkompressibel angenommen. Für die Geschwindigkeits- und Temperaturverteilung wurde eine geschlossene Form der Lösungen erhalten.

Die Anwendung der Lösung auf die Gefriertrocknung zeigt, dass unter besonderen Bedingungen 5 bis 40 Prozent der Energieübertragung durch Konvektion an der Oberfläche des Produkts erfolgt. Wärmestrahlung ist für den Rest der Wärmeübertragung verantwortlich.

ТЕПЛО-И МАССОПЕРЕНОС В ПОЛЧПОРИСТЫХ КАНАЛАХ С ПРИМЕНЕНИЕМ СУБЛИМАЦИОННОЙ СУШКИ (ЗАМОРАЖИВАНИЕМ)

Аннотация—Выполнено аналитическое исследование переноса тепла и количества движения при течении бинарной смеси газов в канале между параллельными пластинами, где на одной стенке присходит вдув массы. Температура стенок различна и применяется сублимационная сушка. Используются интегральные уравнения неразрывности, количества движения и энергии для определения распределений скорости, давления и температуры. Предполагается, что течение стационарное, ламинарное и несжимаемое. Получены решения в замкнутом виде для распределений скорости и температуры.

Применение решения к случаю сублимационной сушки показывает, что при типичных условиях от 5 до 40% энергии передаются к поверхности продукта конвекцией. Остальное количество тепла передаётся излучением.